Naval Research Laboratory

Stennis Space Center, MS 39529-5004

NRL/MR/7442--98-8092

Validation of the Semi-Empirical Longshore Current Model

DENNIS L. LUNDBERG
K. TODD HOLLAND
JOHN CASEY CHURCH

Mapping, Charting, and Geodesy Branch
Marine Geosciences Division

February 25, 1999

Approved for public release; distribution is unlimited.

REPORT DOCUMENTATION PAGE

Form Approved
OBM No. 0704-0188

1. AGENCY USE ONLY *(Leave blank)*

2. REPORT DATE
February 25, 1999

3. REPORT TYPE AND DATES COVERED
Final

4. TITLE AND SUBTITLE
Validation of the Semi-Empirical Longshore Current Model

5. FUNDING NUMBERS
Job Order No. 74-6620-08
Program Element No. 0602435N
Project No.
Task No.
Accession No.

6. AUTHOR(S)
Dennis L. Lundberg, K. Todd Holland, and John Casey Church

7. PERFORMING ORGANIZATION NAME(S) AND ADDRESS(ES)
Naval Research Laboratory
Marine Geosciences Division
Stennis Space Center, MS 39529-5004

8. PERFORMING ORGANIZATION REPORT NUMBER
NRL/MR/7442--98-8092

9. SPONSORING/MONITORING AGENCY NAME(S) AND ADDRESS(ES)
Office of Naval Research
800 N. Quincy Street
Arlington, VA 22217–5660

10. SPONSORING/MONITORING AGENCY REPORT NUMBER

11. SUPPLEMENTARY NOTES

12a. DISTRIBUTION/AVAILABILITY STATEMENT
Approved for public release; distribution unlimited.

12b. DISTRIBUTION CODE

13. ABSTRACT *(Maximum 200 words)*

A previously developed semi-empirical longshore current model that does not rely upon bathymetry was tested to determine the validity of the model on both planar (Santa Barbara, CA) and barred beaches (DUCK94 experiment). The only inputs are wave breaker height, wave breaker angle, and surf zone width. The model was further evaluated to determine conditions under which it failed. The results indicate that the model can be generally applied without a detailed knowledge of the bathymetry. Under most environmental circumstances, the percent error was 14–22%. Based on the DUCK94 data set, the model did not perform as well when wind forcing or alongshore pressure gradients appeared to be forcing the longshore current. Nevertheless, 84% of the predictions had a normalized average error of 50% or less, indicating the model is reasonably robust.

14. SUBJECT TERMS
longshore current, surf zone, mine warfare, amphibious warfare

15. NUMBER OF PAGES
34

16. PRICE CODE

17. SECURITY CLASSIFICATION OF REPORT	18. SECURITY CLASSIFICATION OF THIS PAGE	19. SECURITY CLASSIFICATION OF ABSTRACT	20. LIMITATION OF ABSTRACT
Unclassified	Unclassified	Unclassified	SAR

NSN 7540-01-280-5500

Standard Form 298 (Rev. 2-89)
Prescribed by ANSI Std. Z39-18
298-102

Validation of the Semi-Empirical Longshore Current Model

Dennis L. Lundberg

K. Todd Holland

John Casey Church

INTRODUCTION

The Surf Zone/Mine Interaction project was designed to study and predict the motion of mobile mines within the surf zone. A key factor to predict mine migration in the surf zone is the longshore current. Therefore, one of main the goals of the Surf Zone/Mine Interaction project was to develop a simple longshore current model with inputs that can be directly measured and/or estimated in the field and is not dependent on detailed knowledge of the bathymetry. This has been done and is described in the previous report (Lundberg et al 1997). Longshore current velocity as a function of distance offshore, $\hat{v}(x)$ is modeled with the following three inputs: wave breaker height, wave breaker angle, and the surf zone width. Equation (1) is the model algorithm.

For $0 < \frac{x}{x_b} \leq 1$:

(1a) $$\hat{v}(x, x_b, H_b, \alpha_b) = \left(-32.30\left(\frac{x}{x_b}\right)^{1.057} + 43.78\left(\frac{x}{x_b}\right)\right)\left(\sqrt{gH_b}\sin\alpha_b\cos\alpha_b\right)$$

For $1 < \frac{x}{x_b} < \infty$:

(1b) $$\hat{v}(x, x_b, H_b, \alpha_b) = \left(0.69\left(\frac{x}{x_b}\right)^{-2.557}\right)\left(\sqrt{gH_b}\sin\alpha_b\cos\alpha_b\right)$$

where x is offshore distance, x_b is the observed surf zone width, H_b is the observed breaker height, and α_b is the observed breaker angle. The model is semi-empirical and based upon the theoretical developments of Longuet-Higgins (1970a and 1970b) and of Komar (1979). Although derived for a plane beach, the model was found applicable to a barred beach using empirical coefficients determined from data collected during the DELILAH experiment (Birkemeier, 1991) at the U.S. Army Corps of Engineers Field Research Facility, Duck, North Carolina.

The results from the Delilah data showed that the mode of the model error was approximately 15%. The majority of the errors were less than 30%. The model predicted the location of the maximum current within 20 m on average. A linear regression of the predicted maximum current and the measured maximum current gave a slope of 1.18 which is quite close to values reported in the literature for planar beaches.

The goal of this report is to test the model with other data sets to evaluate its applicability in operational conditions at other beaches. In particular, we wanted to determine whether our supposition that the model can be applied to both planar and barred beaches (in other words, without regard to detailed bathymetry) is correct. The data used were from Santa Barbara, CA collected as part of the National Sediment Transport Study (NSTS) and from the DUCK94 Experiment at Duck, NC. In addition, it was desirable to evaluate errors in the model predictions under a wide range of forcing conditions to ascertain its strengths and weaknesses.

EXPERIMENTAL DESCRIPTION

Santa Barbara

The planar beach subset of the data used in the model validation were from Leadbetter Beach in Santa Barbara, CA collected on 2,4,5,6,8, and10 February as part of the National Sediment Transport Study conducted in January -February, 1980. Leadbetter Beach is oriented east-west with a simple monotonic profile. Swell waves were narrow banded in frequency and direction during the times used in this analysis. (Gable, 1981). The cross-shore array consisted of eleven Marsh-McBirney electro-magnetic current meters and six pressure transducers (Gable, 1981). The current meters were placed within 1 m of the bottom. The data were sampled at 2 Hz from which one hour mean cross-shore profiles were calculated. An offshore array of four pressure sensors at the 9 m depth was used to determine the offshore wave height (H_o) and direction (α_o). Winds were weak during this time such that locally generated wind waves were not present (Wu et al., 1983).

DUCK94

The Duck94 experiment was a follow-up to the DELILAH experiment. The core of the DUCK94 measurements were made during the months of August and October, 1994, although various investigators conducted experiments from June through December. The instrumentation relevant to this analysis included a cross-shore array of fifteen electro-magnetic current meters which provided measurements of the cross-shore profile of the longshore current ($v_{obs}(x)$). The current meters are mounted near the bottom with the assumption that the longshore current had no vertical shear (i.e., constant with depth). The significant offshore wave height (H_o) was determined from a linear array deployed at the 8 m depth contour while the wave angle (α_o) of the predominant wave period also given by this array was used to estimate the wave breaker angle (α_b). The significant wave height measured at the end of the pier was used as the wave breaker height (H_b). This is not unreasonable since data from DUCK94 indicate that the wave height in the very nearshore, but outside the breaker zone, is fairly uniform up to the break point where it rapidly decays due to breaking (e.g. Feddersen et al., 1996; Figure 6). Wind speed and direction were measured by an anemometer located at the end of the pier 19 m above MSL referenced to the 1929 National Geodetic Vertical Datum (NGVD).

Two time periods from DUCK94 were used in the model validation. They were 27 August, 1994 through 17 September, 1994 and 15 October, 1994 through 31 October, 1994. Typically the wave heights at the end of the pier were from 0.5 to 1.0 m during both periods with storm wave heights reaching 2.5 m during the first period and over 3.0 m during the second period. The winds were generally from the east to southwest less than 6 m/sec except during storm events when they were from the north-northwest to the northeast with speeds up to 18 m/sec.

METHODS

The model input parameters are wave breaker height (H_b), breaker wave angle (α_b), and surf zone width (x_b); of which $\hat{\alpha}_b$ and $\hat{x}_b$ were estimated using measurements of offshore wave angles, offshore wave heights, and measured beach slopes. Straightforward relationships were used to provide the best estimate of these input variables as follows.

The estimation of $\hat{x}_b$ for the Santa Barbara Site was calculated from (H_o) and the relationship:

$$(2) \qquad \hat{x}_b = H_o / (\gamma \tan\beta)$$

where $\hat{x}_b$ is the surf zone width, γ is the breaker criterion, and $\tan\beta$ is the bottom slope. The respective values of γ and $\tan\beta$ were 0.43 and 0.042 (Thornton and Guza, 1986). In contrast, a linear relationship between H_o and $\hat{x}_b$ established using DELILAH data (Lundberg et al, 1997) was used to estimate the surf zone width for DUCK94 as:

$$(3) \qquad \hat{x}_b = 95 H_o$$

Using equation (2) implies that, $1/(\gamma \tan\beta) = 95$. For values typical of Duck, $\tan\beta = 0.02$ which gives $\gamma = 0.53$, equation (3) appears to be adequate.

The significant wave height (H_s) for each pressure sensor in the cross-shore array at Santa Barbara was calculated from the wave energy spectra of each sensor to provide a cross-shore profile of the wave height. The wave breaker height H_b was taken to be the largest wave height measured by the pressure sensors from the cross shore array. The depth of breaking h_b was taken as the depth of that sensor measuring the largest wave height (corrected for tide). For the DUCK94 data set, equation (4) was solved for the depth of breaking, h_b, where $\hat{x}_b$ was determined from equation (3).

$$h_b = \hat{x}_b \tan\beta \qquad (4)$$

The breaker wave angle ($\hat{\alpha}_b$) for both experiments was estimated using Snells Law (equation 5)

$$\frac{\sin\alpha_b}{\sin\alpha_o} = \frac{\sqrt{h_b}}{\sqrt{h_o}} \qquad (5)$$

to refract the wave angle determined by the measurements from the offshore arrays to the estimated depth of breaking (h_b). The wave angle measured at the offshore arrays is α_o and h_o is the water depth.

Data were screened to remove those profiles where current reversals occurred in the cross-shore (i.e., current shear) and where not all of the pertinent data were available (i.e., wave height and breaker angle). The number of valid runs for Duck was 1266 (of 3120) and for Santa Barbara, 24 (of 24).

The normalized percent error (equation 6) was computed for each predicted profile using the measured data.

$$err_j = \left(\frac{1}{NO}\sum_{i=1}^{NO} |\hat{v}_i - v_{obs,i}| / |\hat{v}_{max,j}|\right) \bullet 100 \qquad (6)$$

where NO is the number of measurements in profile j; $\hat{v}_i$ and $v_{obs,i}$ are the respective estimated and measured longshore currents at the cross-shore location i of profile j; and $\hat{v}_{max,j}$ is the predicted maximum in the longshore current. This particular formulation for the calculation of the error was used because it places greater weight on the currents within the surf zone rather than the smaller currents outside the surf zone. This leads to a smaller percent error. To ensure that this formulation did not present an overly optimistic result, the root mean square error (RMS) for each profile was calculated (equation 7).

$$(7) \quad rms_j = \left(\frac{1}{NO} \sum_{i=1}^{NO} (\hat{v}_i - v_{obs,j})^2 \right)^{\frac{1}{2}}$$

RESULTS

NTSB Santa Barbara, CA

Figure 1 is a histogram of results for the model comparison with the data collected from Santa Barbara, CA. The percent error ranged from 6% to 44% with the majority less than 30%. The modal percent error is between 14% and 18% while the mean value was 19%. This compares favorably with the DELILAH data set where the majority of the errors were also less than 30% and the modal value was between 14% and 18%. The RMS error (Figure 2) has a mean value of 10.6 cm/sec and the mode is 8.0 cm/sec. To summarize, the percent errors relative to the maximum current are less than 20% and the absolute differences are less than 10 cm/sec. The conclusion is that the model performed reasonably well for this data set.

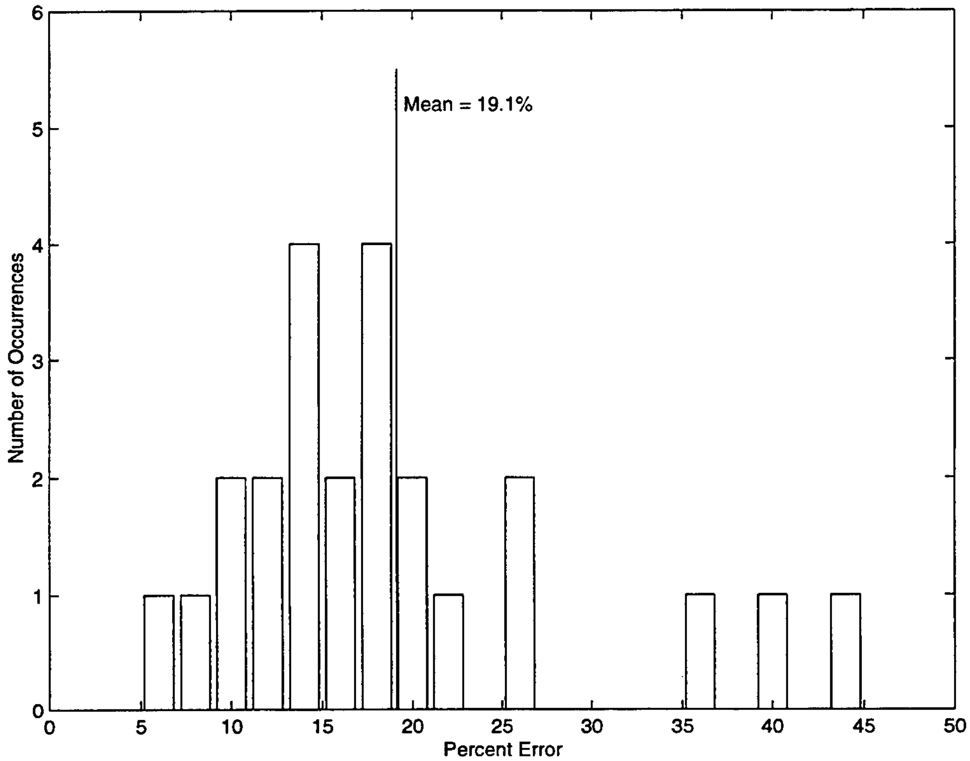

Figure 1. Histogram of the normalized percent error for the Santa Barbara data.

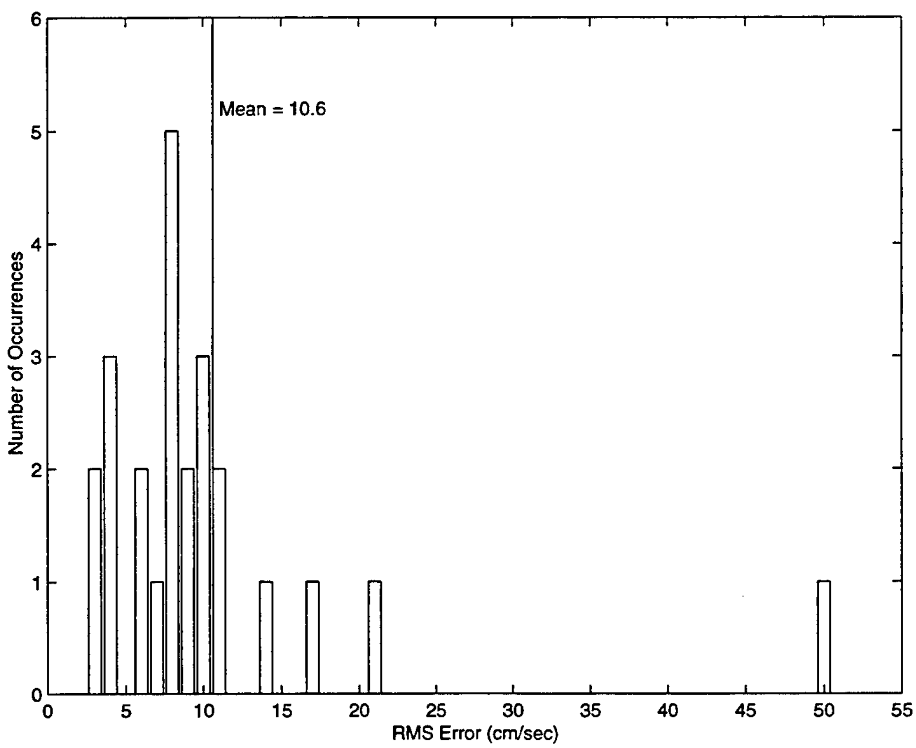

Figure 2. Root mean square (RMS) error for Santa Barbara.

One of the major sources of error in the model can arise in the prediction of the maximum current (equation 7). Figure 3 is a comparison between the maximum longshore current predictor (equation 7) and the measured maximum longshore current where C=1.18 from the DELILAH data set. (see Fig. 3)

$$v_{max}(H_b, \alpha_b) = C\sqrt{gH_b}\sin\alpha_b\cos\alpha_b \quad (7)$$

A linear regression of the predicted and the measured maximum current gave a correlation coefficient of 0.9 and accounted for 80.5% of the total variation at a confidence level of 95%. t. The coefficient (C) in equation (7) was re-evaluated with this data and found to

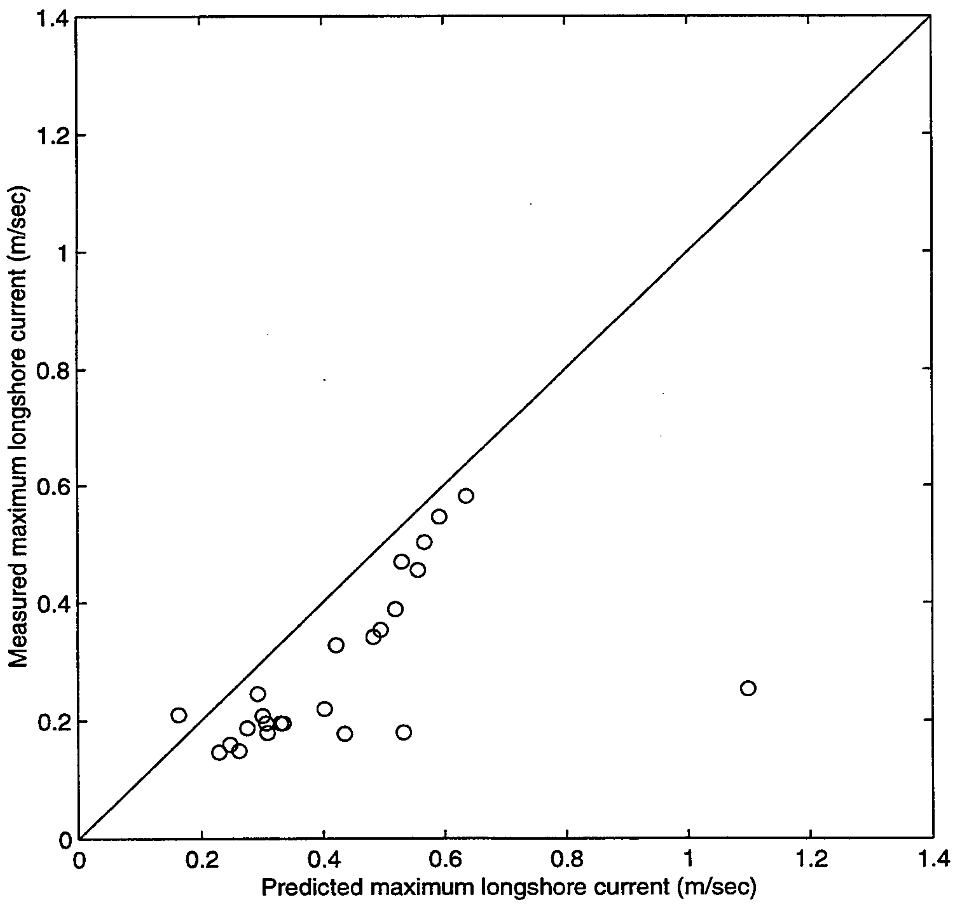

Figure 3. Plot of the estimated maximum current (equation 7) vs the measured maximum current for Santa Barbara. Solid line is a 1:1 relation between measurements and equation (7).

be 0.73 ± 0.13. In general, the trend of the data follow the slope of the predictor but are below the line, or the model tends to over predict the maximum current. Further, because the predicted longshore current profile is scaled by the predicted maximum current, one would expect that for this data set the predicted profile would generally be greater than the measured data which is seen in Figure 4.

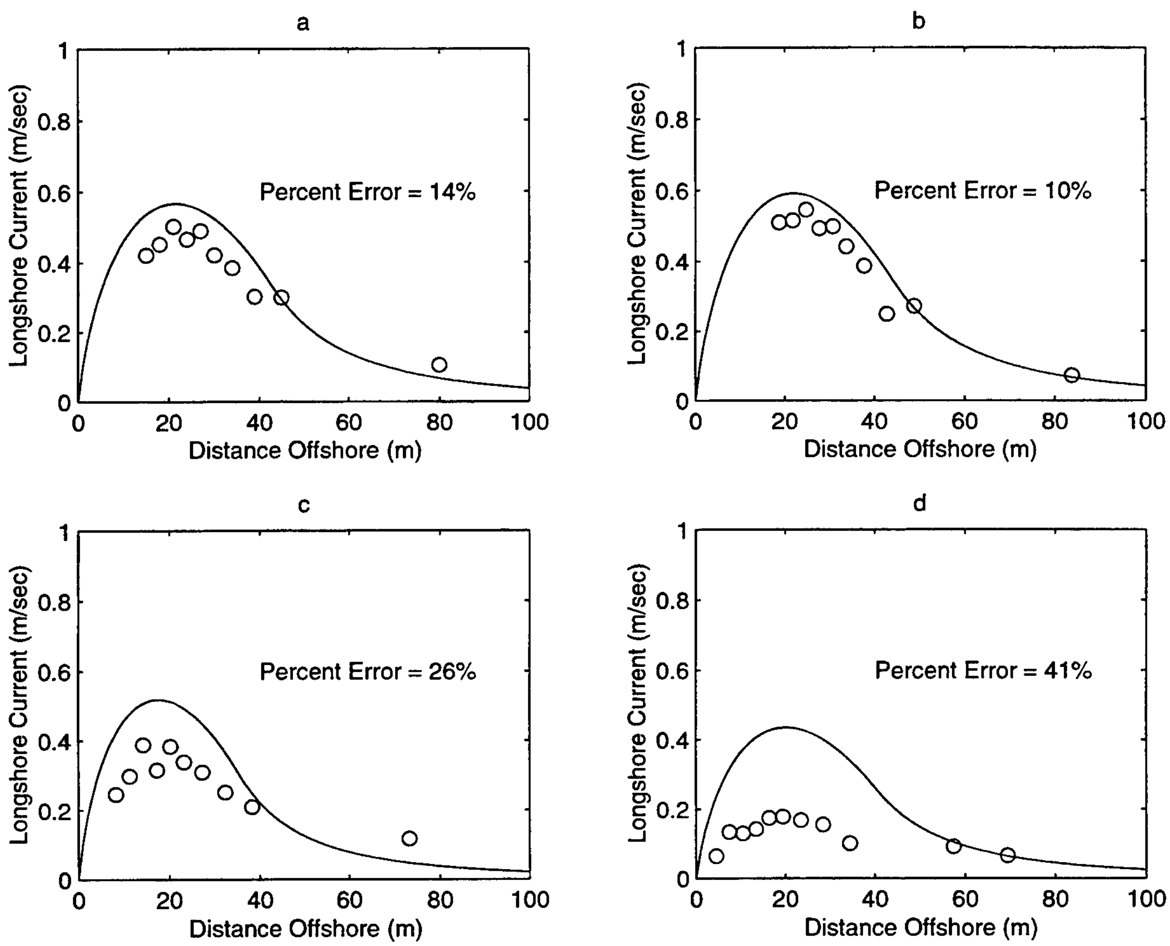

Figure 4. Plot of the predicted (line) and measured (circles) longshore current for Santa Barbara.

Measured and predicted locations of the maximum current are shown in Figure 5. In general, the model places the location of the maximum current closer to shore than the measured, with the difference between the predicted and measured values, in most cases, less than 10 m.

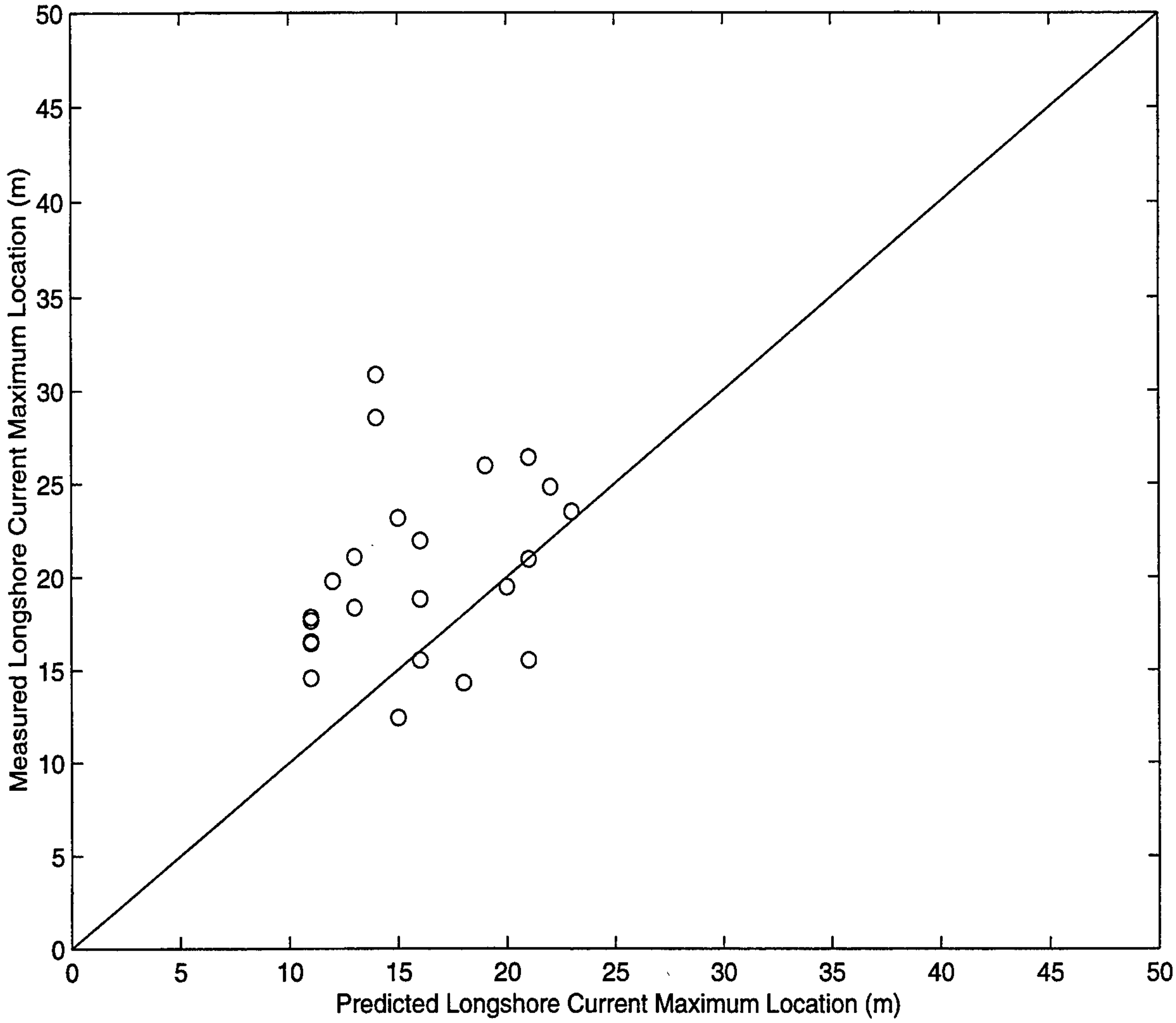

Figure 5. Difference between the predicted and measured location of the maximum current for Santa Barbara.

Duck, NC DUCK94

The data set from the DUCK94 experiment is much larger than those from either the DELILAH experiment or the NSTS study at Santa Barbara. The overall results of the model comparison (equation 6) are shown in Figure 6. The modal value is 22% which is slightly greater than the results from the DELILAH and Santa Barbara data sets. There is wider spread to the error yet the great majority (84%) of the errors fall below 50%. The mean error was 62%. The group at 200% (approximately 40 runs) are primarily related to those runs where the predicted longshore current was small but the measured values were large. These will be discussed in a later section. The RMS errors are shown in Figure 7.

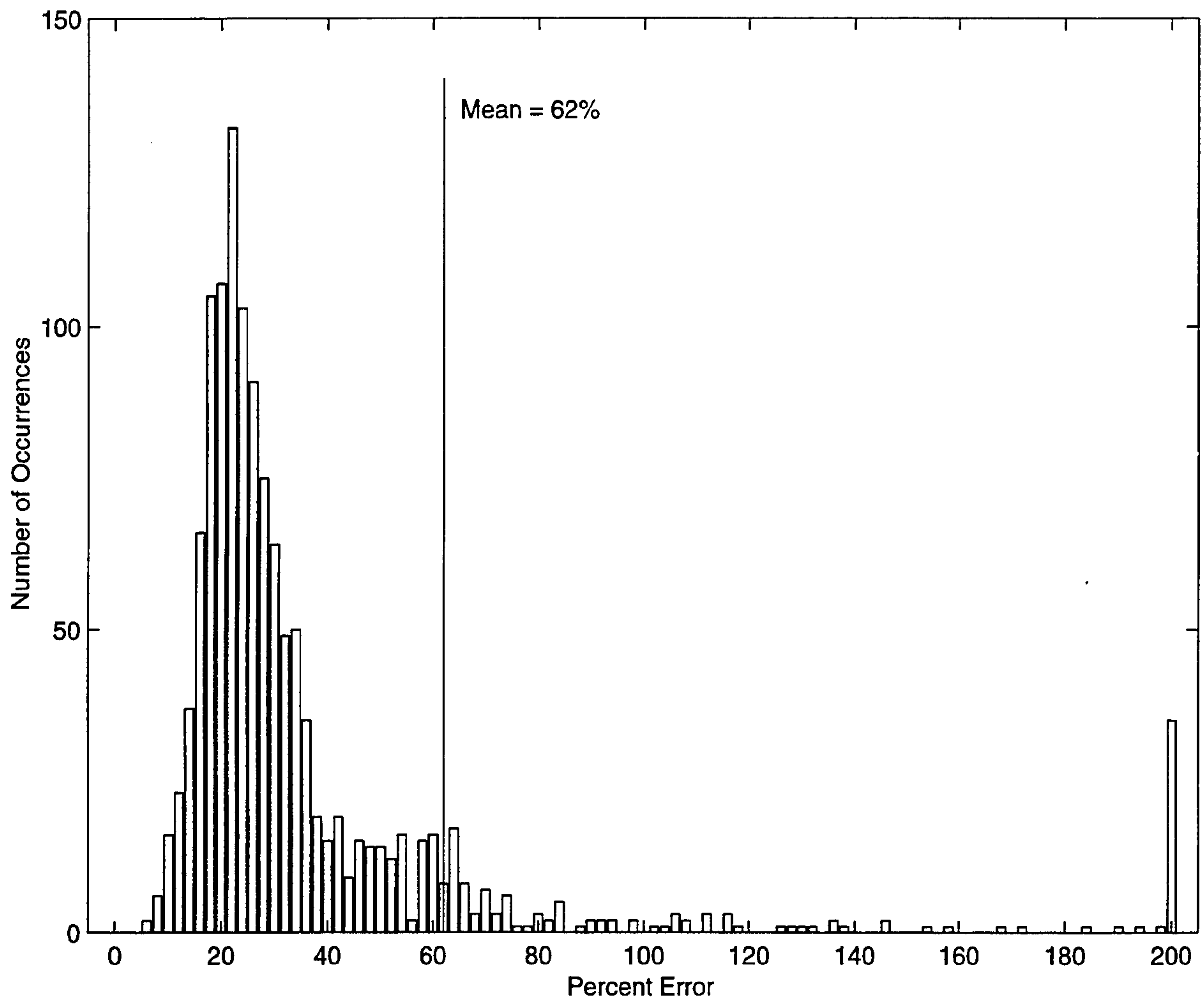

Figure 6. Histogram of the normalized average error for the DUCK94 data.

The mean value is 21.1 cm/sec and the mode is 8.0 cm/sec. While the mean value is greater than the Santa Barbara results, the mode is the same. Considering the simplicity of the model, the overall results are quite good.

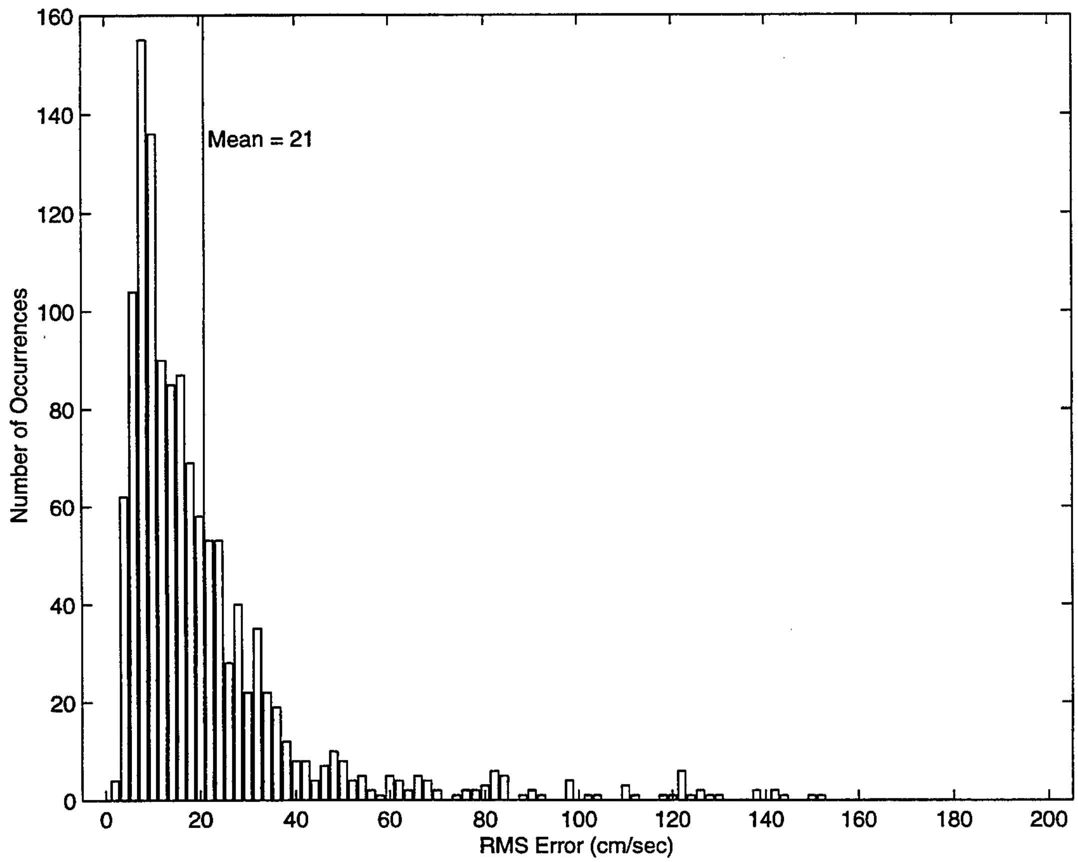

Figure 7. The RMS error for the DUCK94 data.

Figure 8 is a scatter plot of the predicted maximum current (equation 7) and the measured maximum current. Outliers were grouped such that data points marked with the + symbol are those cases where the measured maximum current flowed opposite to the predominant wave forcing in the presence of strong winds while the points marked with the * symbol are those cases where the percent error exceeded 100%. These cases will be discussed in detail later. A linear regression (all the data) of the estimated and the measured maximum longshore current had a correlation coefficient of 0.99 and accounted for 97.6% of the total variation at a confidence level of 95%. The value of C that best fits the equation (7) for DUCK94 is 0.59 ± 0.02. These results and those from

Santa Barbara suggest that the constant (C = 1.18) is too large; however, using a smaller value for C would not agree with prior theory and observation (Komar, 1979 and Lundberg et al; 1997).

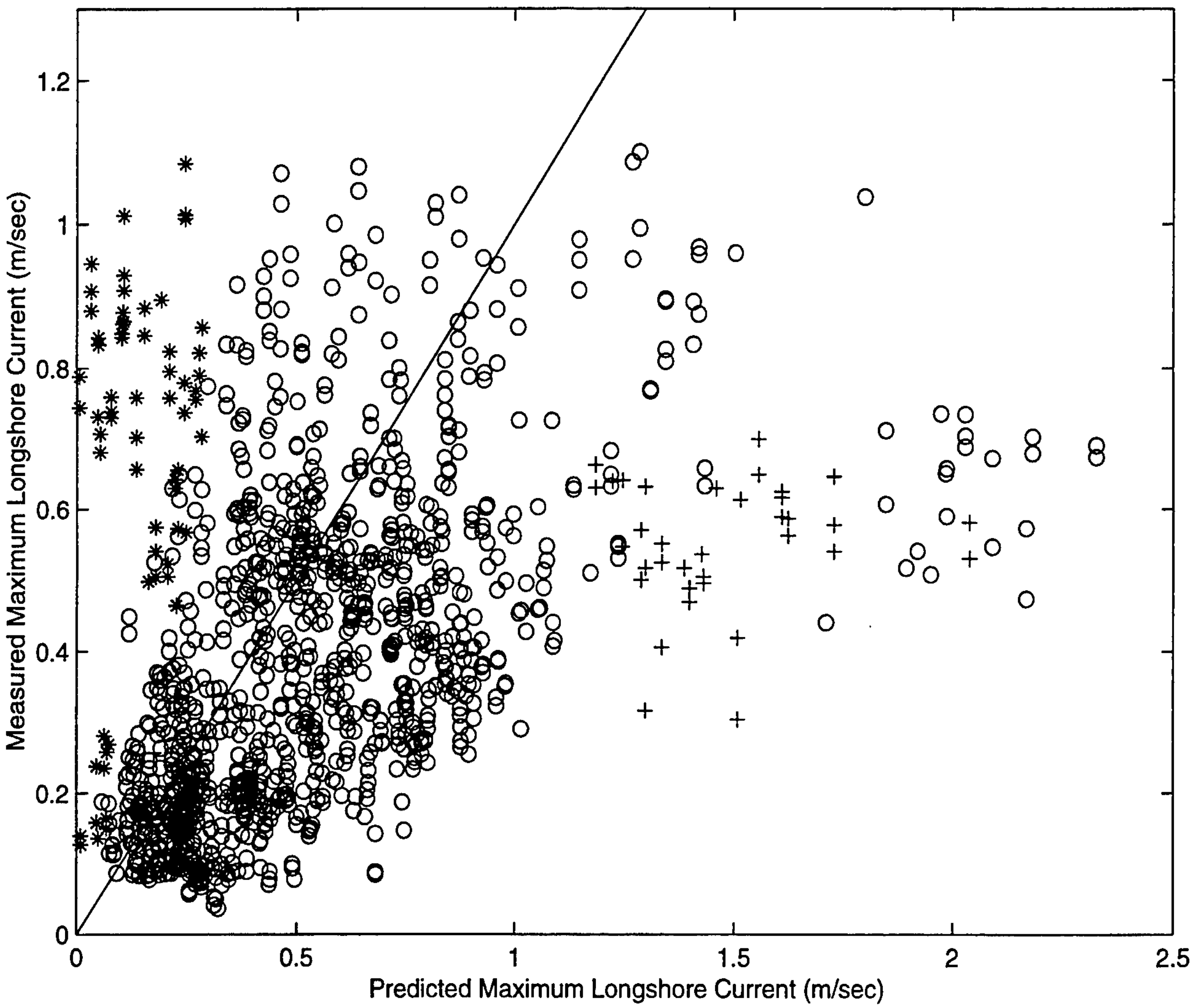

Figure 8. Plot of the predicted maximum current (equation 7) vs. measured maximum current for DUCK94. The solid line is a 1:1 relation between predicted and measured longshore current maximum.

Examples of the predicted longshore current (line) and the measured longshore cur-

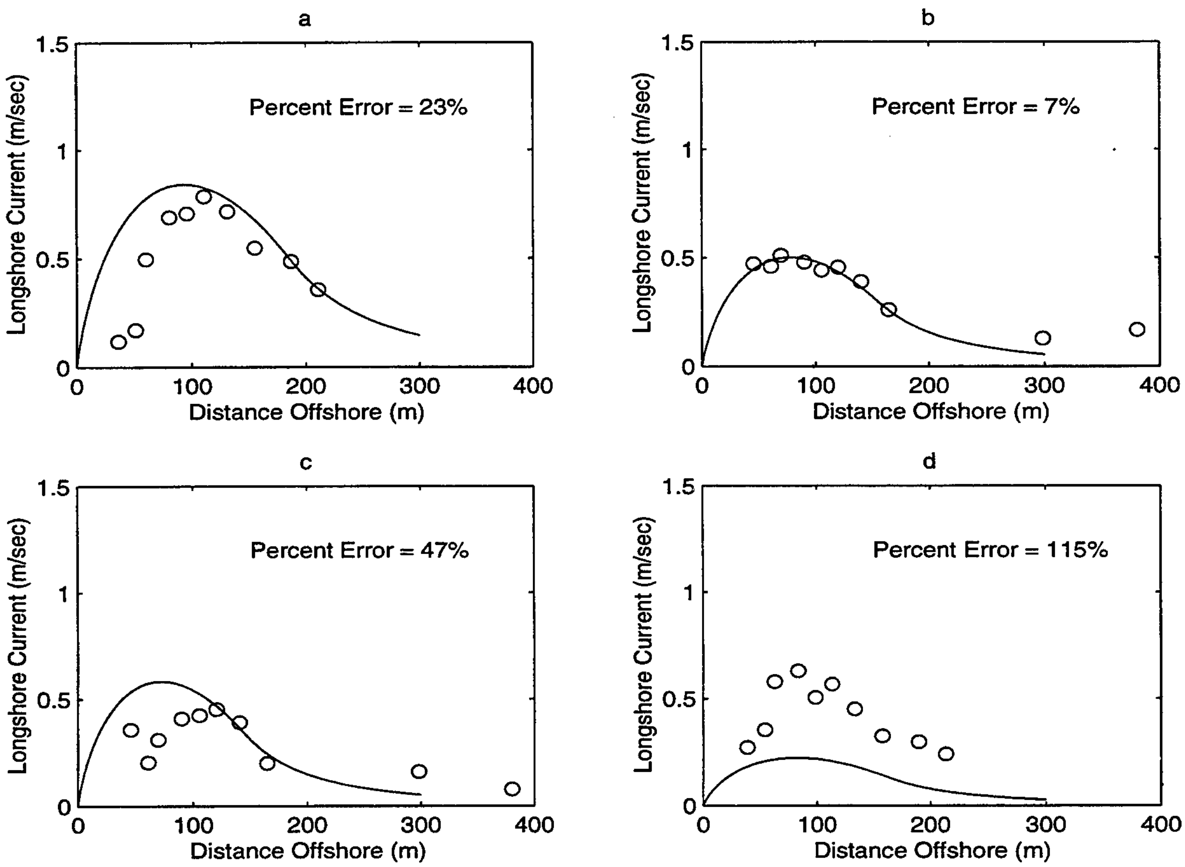

Figure 9. Plot of the predicted (line) and measured (circles) longshore current for DUCK94

rent (circles) versus distance offshore are given in Figure 9. Panel (a) is an example of a profile where the percent error is near the mode while panel (b) is one of the better predictions. Panel (c) is an example of a profile outside the main grouping in Figure 7 and panel (d) is an example from the subset where the percent error exceeded 100%. Since panel (a) represents the majority of the predictions, the model appears to perform reasonably well.

Differences in the maximum current location in the cross-shore were also examined. To do so, the Duck94 data were further screened to select profiles that had a sufficient number of working sensors to define the general profile and where the maximum current was at least 0.3 m/sec. The maximum current constraint generally excluded profiles that were nearly flat (i.e., no structure). In addition, those profiles in which the maximum was measured near the shoreline were excluded. This more stringent selection resulted in 511 profiles. Figure 10 depicts the results. There is considerable scatter to the data about the perfect fit line. The average absolute difference between the predicted and measured location of the maximum current was approximately 30 m with approximately 60% of the runs less than the mean.

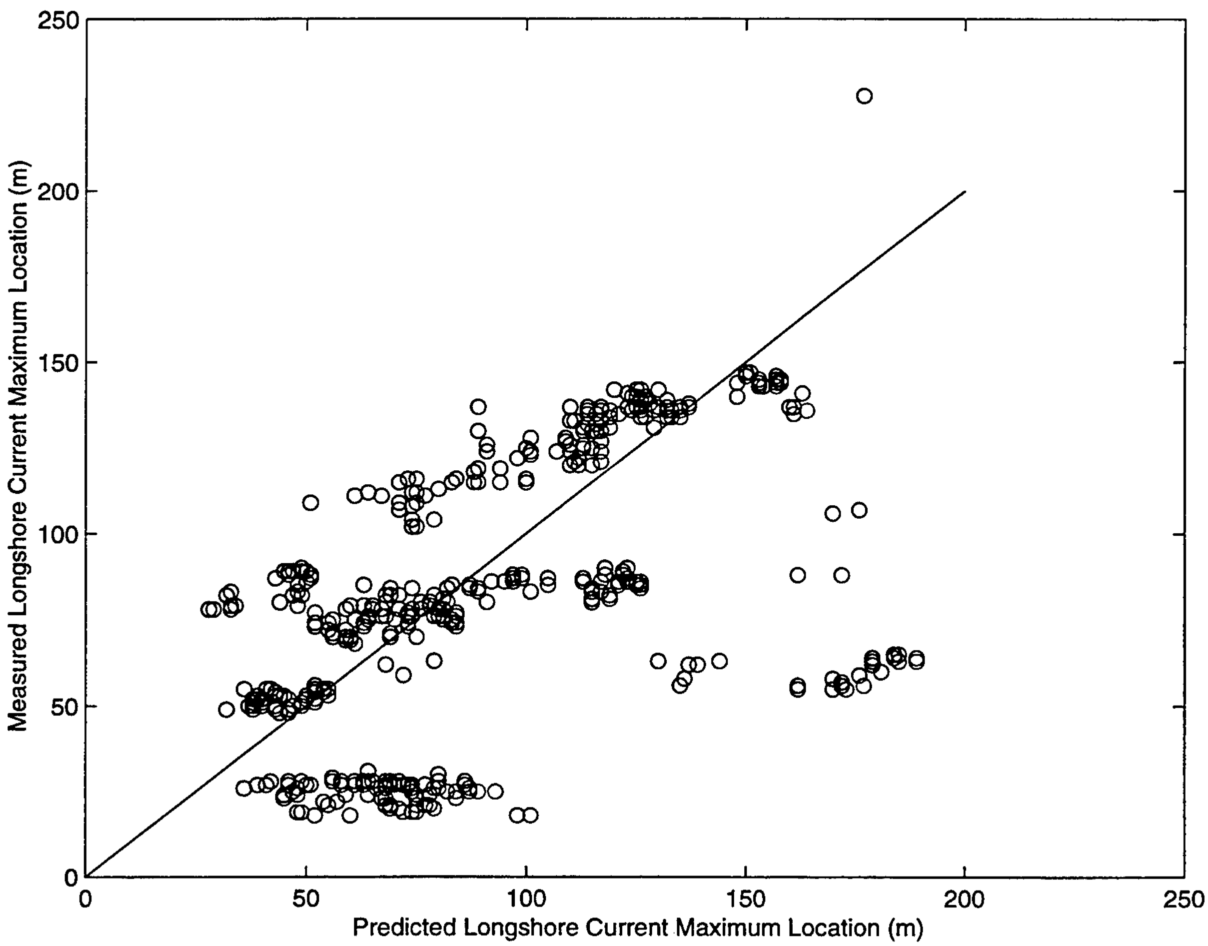

Figure 10. Differences between the predicted and measured maximum current location for Duck94 (location measured from shore).

The authors believe that one likely cause for these differences between the model predictions and observations is the horizontal mixing coefficient (P). Longuet-Higgins (1970b) showed that as P increases, the location of the maximum current normalized by the surf zone width moves closer to the shoreline. In the Longuet-Higgins (1970b) formulation, P is a function of the beach slope and the bottom drag coefficient (c_f). $P = 0.37$ in this model which puts the maximum location near the mid-surf position (Longuet-Higgins, 1970b, Fig. 3). A fixed P implies that the cross-shore location of the maximum current normalized by the surf zone width is constant and c_f is constant both spatially and temporally. Church and Thornton (1993) showed that c_f within the surf zone may be a function of turbulence due to wave breaking which is time varying. Garcez et al (1998) showed that the time averaged c_f varies across the surf zone. Since c_f can vary both temporally and spatially, P also can vary accordingly. Hence, there are conditions when the value of P used in the model is not correct which can result in errors in the predicted location of the current maximum. However, the mid-surf position of the current maximum is generally consistent with observations (Komar and Oltman-Shay,1990). In a broad sense, the mid-surf position of the maximum current best describes what is observed in nature as can be seen in the overall prediction error (Figures 6 and 7). Hence, the varying P and its impact on the location of the current maximum does not appear to have a large impact on the overall prediction error.

Environmental Factors

Environmentally related errors can arise from two very general categories. One is errors in the model input parameters and the other is processes that affect the longshore current and are not accounted for in the model (e.g., wind forcing or alongshore pressure gradients). Accordingly, linear regressions were done between the percent error and the different model input parameters to determine if the errors were correlated with the inputs. Hubertz (1986) and Xu and Wright (1998) have shown that wind forcing may be a significant factor in driving nearshore currents at Duck, NC. Since wind measurements were available from DUCK94, they were included in this portion of the analysis. The correlations were tested for significance at the 95% confidence level.

Table 1: Santa Barbara

	α_b	H_b	$\hat{x}_b$	Wind Speed
r	0.36	0.11	0.10	N/A
% Variance	12.8	1.0	1.0	N/A
Significant	No	No	No	N/A

Table 1 summarizes the results for the Santa Barbara data. Wind data were not available for Santa Barbara. There was no significant correlation between the model input variables and the model errors which indicates the sources of error in the predictions may be from factors not considered by the model. Table 2 summarizes the results of a linear regression of the model inputs and wind speed to the percent error for DUCK94. Table 2 shows that for DUCK94 the errors induced by the input parameters contributed to less than 2% of the variance. The same can be said of errors induced by winds. These results show that, in general, the input variables contribute little to the observed error indicating that with respect to the input variables, the model is robust. It also shows that the wind forcing has very little overall effect on errors in the longshore current predictions.

Table 2: DUCK94

	α_b	H_b	$\hat{x}_b$	Wind Speed
r	0.11	0.12	0.13	0.13
% Variance	1.2	1.5	1.7	1.4
Significant	Yes	Yes	Yes	Yes

Typically, the above generalizations are true. However, there appear to be particular conditions when they do not hold. These conditions can be seen in the outliers in Figure 8 which are subdivided into two cases. The first case consists of those runs where wave forcing was opposite to the direction of the maximum current, wave angles were > 10^o, and winds in excess of 8 m/sec (15 knots). These are the data points in Figure 8 with the + labels. There were 43 occurrences in this category or about 3% of the data. The second case was runs where the percent error for each profile exceeded 100% and are labeled with * symbol in Figure 8. This produced 66 occurrences or 5% of the data. As will be seen below, Case I occurs when strong winds opposed the oblique wave forcing, and Case II errors occur when the primary wave approach was nearly shore normal accompanied by strong winds.

Case I

The time period when the Case I errors occurred was from 15-16 October, 1994 and are coincident with the passage of a storm. In the majority of the Case I runs (35), the wave breaker height was between 2.5 to 3.2 m and the remainder (8 runs) were less than 0.5 m. The primary wave breaker angles ranged from 10 - 19^o and showed wave propagation to the north. For these wave conditions (generally large waves and large angles) one would expect strong longshore currents to the north. But, in all cases the longshore current flowed to the south in opposition to the predominant wave forcing.

An examination of the wind direction and speed for these occurrences showed that in all runs the winds were from the north to the northeast with speeds of 10 m/sec to 18 m/sec (19 - 35 knots). The wind forcing from the northerly quadrant is similar to the conditions described by Xu and Wright (1998). They showed a correlation between currents measured in the nearshore and wind stress from storm related northeast winds, but no correlation with southerly winds. They speculated that the strong "downwelling" northerly winds exerted greater stress on the sea surface than the southerly "upwelling" winds. This is reasonable since northerly winds associated with a storm passage tend to be a descending (downwelling) stable air mass made up of cold, dry air. Southerly winds on the other hand tend to be warm moist air that is unstable which rises (upwells). The result is that the northerly winds exert greater stress on the water surface. In addition, the northerly winds tend to enhance the coastal plume from the Chesapeake Bay (Ludwick, 1978). The coastal plume may be an additional forcing component to the south. The measurements of Xu and Wright (1998) were not within the surf zone but they indicate that wind stress may be a significant component of the forces acting within the surf zone under certain conditions. Accordingly, wind effects are examined as a possible source of prediction errors in this case.

The linear correlations between the percent error and the most important forcing parameters are shown in Table 3. From these results, it is clear that wind has a signifi-

Table 3: DUCK94

	α_b	H_b	Wind Speed
r	0.56	0.62	0.38
% Variance	32	38	15
Significant	Yes	Yes	Yes

cant but modest contribution to errors in the longshore current prediction while the wave height and wave breaker angle account for more of the variance in the prediction errors. The Case I errors are due to wind forcing in two ways. The first is a result of currents generated directly by wind stress. The second is that the strong winds are probably producing local wind waves approaching from the north with a large angle to the beach. This local, secondary wave train approaching the beach from the north in combination with the wind stress, may be sufficient to overcome the wave forcing from the primary waves thus forcing the longshore current to flow south in opposition to the primary wave forcing. This may explain the correlations between α_b and H_b with the prediction error as well as the correlation of the wind speed to the prediction error.

Case II

This case is when the normalized percent error (Figure 5) was greater than 100%

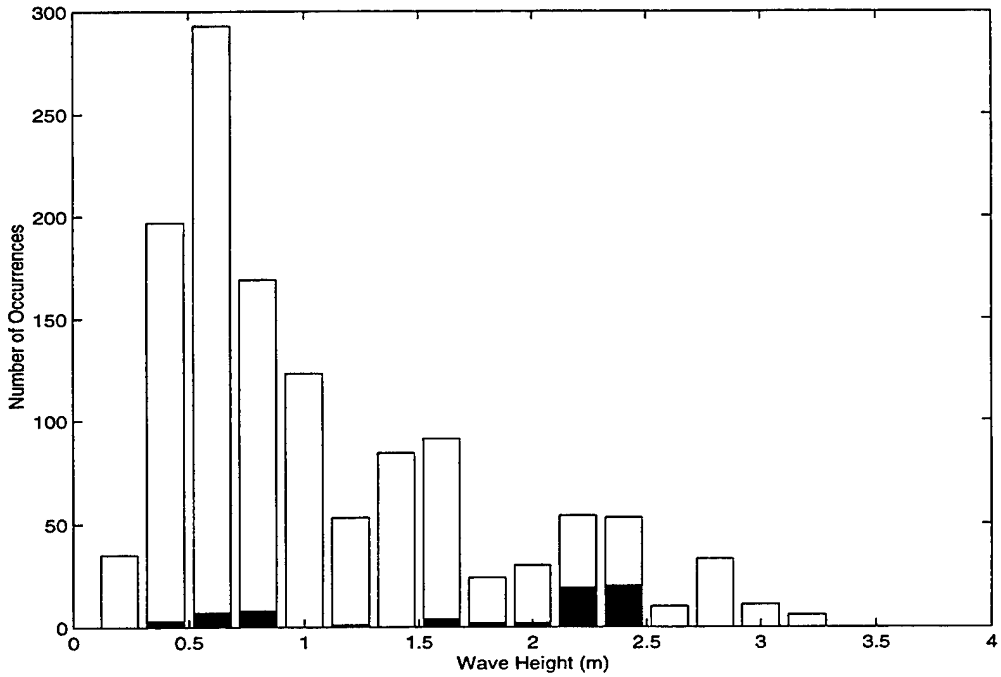

Figure 11. Wave heights for Case II errors (filled) and all data (clear).

(data in Figure 8 denoted by the * symbol along the ordinate axis). The majority of the occurrences (57 of 66) occurred between 2200 02 September and 1834 07 September during which a storm passed through the study site. Figure 11 indicates that the wave breaker heights were generally greater than 1.5 m (47 of 66 runs) with small wave angles ($< 5^o$) to the north in 60 runs (Figure 12).

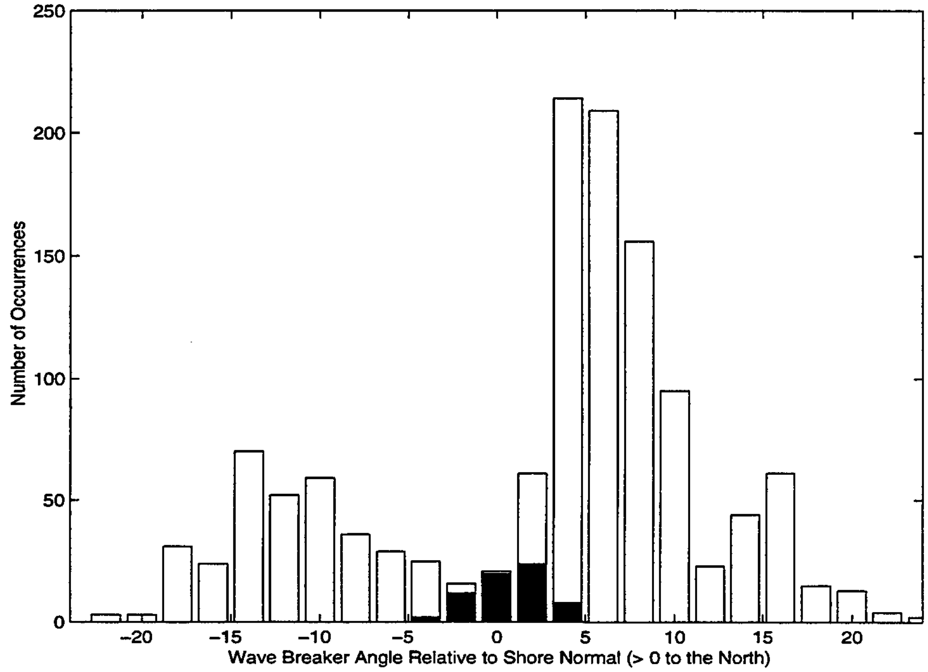

Figure 12. Histogram of the wave breaker angle for Case II errors (filled) and all data (clear) for DUCK94.

In general, the model predicted low longshore currents (<0.3 m/sec) due to the small wave angles. Nevertheless, the measured currents were primarily between 0.5 to 1.1 m/sec to the south, indicating that some other process is forcing the longshore current. Figures 13 and 14 depict the wind direction and speed, respectively.

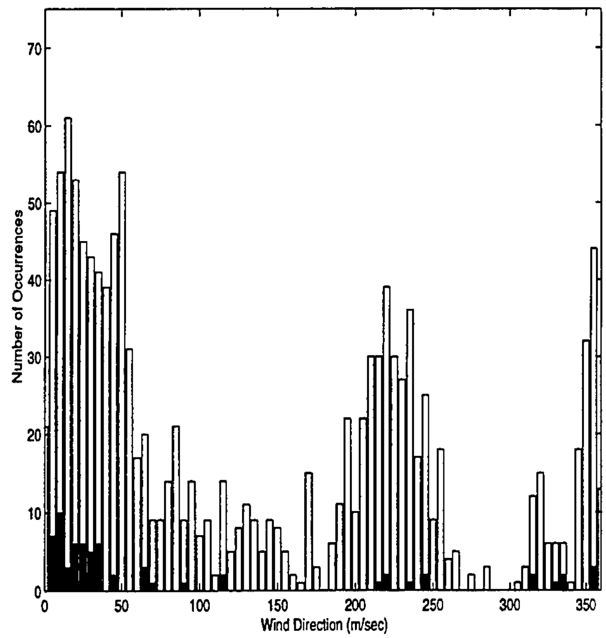

Figure 13. Wind direction for Case II errors (filled) and all data (clear) for DUCK94.

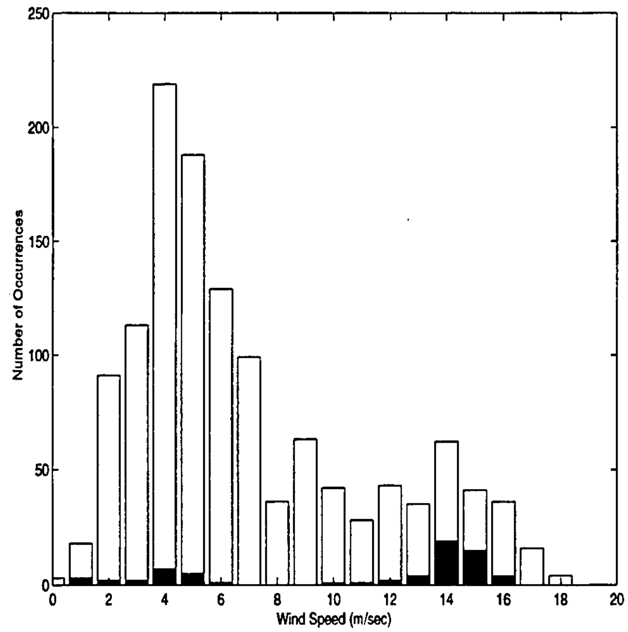

Figure 14. Wind speed for Case II errors (filled) and all data (clear) for DUCK94.

The wind was from the northern quadrant for 54 runs and was in excess of 10 m/sec for 45 runs. Given the conditions of weak wave forcing to the north and strong winds from the north (forcing to the south) and currents flowing to the south, one might expect that the winds and/or secondary waves may be opposing the longshore current. Table 4 summarizes the results of linear regressions of the wave forcing variables and wind speed with the percent error. The results of a linear regression of the wind speed vs. the normalized percent error showed no significant correlation. There also was no correlation

Table 4: DUCK94

	α_b	H_b	Wind Speed
r	0.33	0.18	0.20
% Variance	11	3.4	4.2
Significant	Yes	No	No

between H_b and the percent error and a small correlation between α_b and the percent error at the 95% confidence level. In Case II, the correlations are either small or not significant indicating that there are probably other processes affecting the longshore current that are not accounted for in this simplistic model.

We can speculate that alongshore variations in pressure gradients due to variations in wave set-up may be responsible for the observed errors. Alongshore variations in wave set-up can be the result of subtle variations in bathymetry in the alongshore. Komar (1971) conducted a wave basin study which suggested that the alongshore variations in wave set-up due to a cuspate shoreline may have been sufficient to balance the wave alongshore directed radiation stress from the incident waves. Reiners et al. (1995) presented an argument that alongshore pressure gradients may have produced the observed longshore current in the trough during the DELILAH experiment. They reasoned that alongshore differences in bathymetry resulted in alongshore variations in set-up that enhanced the longshore current in the trough. Putrevu et al. (1995) presented a theoretical approach that takes into account alongshore topographic variations within the surf zone which produced alongshore pressure gradients due to variations in wave set-up. They found that a 10% variation in the bathymetry produced up to a 30% variation in the longshore current about the mean.

The presence of the pier at Duck has produced a general depression in the bathymetry in the vicinity of the pier. As a result, the waves near the pier tend to break further inshore than they would to the north of the pier where the cross-shore array was located. The waves breaking further offshore near the array would produce a greater set-up across the surf zone than near the pier. The result is a pressure gradient that would drive the longshore current to the south. Indeed, the longshore current did flow to the south in opposition to the predominant wave forcing.

Feddersen et al., (1996) reported a similar situation to Case II on October 20 during a storm with large waves and small wave breaker angles. These conditions led to small predicted longshore currents. In contrast, they observed larger than predicted longshore current. Post storm bathymetric surveys indicated longshore bathymetric gradients which can cause alongshore pressure gradients (Putrevu et al., 1995). Feddersen et al., (1996) concluded that the alongshore pressure gradients were responsible for the discrepancy between the predicted and the measured longshore current.

One possible conclusion is that Case II errors are likely due to alongshore pressure gradients produced by alongshore varying wave set-up. The pressure gradients may have been caused by the bathymetric depression caused by the pier or by the reshaping of the bathymetry due to the storm.

DISCUSSION

An underlying assumption of the Semi-Empirical Longshore Current Model is that the incident waves are monochromatic and there are no secondary wave groups (i.e., unidirectional wave approach). The wave angle is determined from the frequency that contains the largest wave energy (i.e. the mode of the energy spectra rather than the mean). When there are strong winds from a direction other than the direction of the predominant wave group, it is likely that a secondary wave group is generated by those winds. The longshore current will respond to the mean forcing which will result in prediction errors in the when secondary wave groups are present. Nevertheless, this simple model predicts the longshore current reasonably well for the planar beach and barred beach used in this analysis. The average error for the longshore current predictions at Santa Barbara were less than 50% for all 24 runs and was less than 30% for 21 runs. The RMS error had a mean value of 10.6 cm/sec with a modal value of 8.0 cm/sec. The percent error from the DUCK94 experiment was under 50% for 84% of the 1266 runs. The mean error was 62% and the mode was 22%. RMS error averaged 21.1 cm/sec with a mode of 8.0 cm/sec.

A closer examination of the largest errors from the DUCK94 data can be broken down into two cases which were associated with the passage of storms and the resultant high waves and winds (primarily from the northeast). These two cases comprised only 8% of the data used in this study. Case I errors can be correlated to wind forcing. The strong winds may also have generated a secondary wave train that opposed the primary incident wave group. Case II errors could not be correlated to wind forcing or to the incident wave forcing, but may be associated with alongshore pressure gradients as discussed above. In both cases, processes that were not accounted for by the model appeared to be responsible for the observed errors. These processes were sufficiently strong to overcome the forcing due to the primary incident waves.

The alongshore pressure gradients required to drive longshore currents are quite small and generally below the resolution of field measurements. The analytical approaches to predict the alongshore pressure gradient require detailed bathymetric measurements. In an operational setting, this level of detail will not be available.

One final mechanism that may affect the longshore current at Duck, NC is the Chesapeake Bay plume that can be deflected to the south by northerly winds (Ludwick, 1978). This may produce a southerly component to the longshore current. There are no data to properly evaluate this hypothesis.

Model Application

Mettlach and May (1997) showed that the Navy Standard Surf Model (NSSM) on a barred beach predicted the wave breaker height, wave breaker angle, surf zone width, and cross-shore distribution of the wave height reasonably well. However, it did not do as well in the prediction of the longshore current. This model tested herein can be used in conjunction with the NSSM to provide better predictions of the longshore current by using the predicted wave breaker height, wave breaker angle, and surf zone width from the NSSM as input variables to this model to provide the longshore current predictions.

The simplicity of this model and the few input parameters required gives it the advantage of ease of use in the field. The wave height, wave angle and surf zone width are parameters that can be visually estimated and input to the model which can be programmed into a hand held computer. This affords a high degree of operational utility to forward deployed forces. However, under these conditions, visual estimates will have large errors that will affect the predictions. For example, Allender and Ditmars (1981, Table I), noted that when visual estimates of the breaker angle could be compared to concurrent measured breaker angles from aerial photographs, the visual estimates were too large. The differences ranged from 6^{o} to 15^{o} which could result in significant errors in the predicted longshore current. A viable means of operationally measuring wave angle and surf zone width is the use of video imagery techniques described by Holland et al. (1997). These methods are readily adaptable to fleet applications either from a fixed shore station or from an airborne platform to measure the surf zone width and the wave breaker angle.

SUMMARY

The results from both a planar beach at Santa Barbara CA and a barred beach at Duck, NC reveal that the majority of the longshore current profile predictions had errors under 50%. The modal values for the errors are 14%-18% for Santa Barbara and 22% for DUCK94. The RMS errors were 8.0 cm/sec for both Santa Barbara and DUCK94 with average RMS errors of 10.6 cm/sec and 21.1 cm/sec respectively. Detailed bathymetry was not required to provide the predicted longshore current. Those results are a good indicator that this model can be operationally applied in forward regions where data such as bathymetry is limited or nonexistent. The only input variables required by the model are H_b, wave breaker height; α_b, wave breaker angle; and x_b, surf zone width. These inputs can be obtained from either visual estimates, remote sensing, or predictions from other models. Video imaging techniques from airborne reconnaissance vehicles or fixed, land based platforms can provide quantified measurements of α_b and x_b. More sophisticated remote sensing techniques also may provide measurements of H_b.

The model only considers the longshore directed momentum flux as the forcing function for the longshore current. It does not consider wind forcing and the forcing due to pressure gradients. The results show that wind forcing and associated local wind waves are a minimal factor. Only about 3% of the time did this appear to be significant (Case I). The Case II errors indicate that some other process may play a significant role in forcing the longshore current. A potential mechanism is alongshore pressure gradients, although there are no data in this study to determine if this is so. Both cases indicated that the model may perform poorly when other processes such as wind forcing or alongshore variations in pressure contribute significantly to the longshore current forcing.

Acknowledgments

Data from Duck94 was provided by Steve Elgar and from Santa Barbara by Joan Oltman-Shay. Without their support, this study would not have been possible.

REFERENCES

Allender, J.H. and J.D. Ditmars, 1981, Field measurements of longshore currents an a barred beach, Coastal Engineering, V. 5, pp. 295-309.

Birkemeier, W.A., 1991, Samson and Delilah at the FRF, The CerCular, CERC-91-1, pp. 1-6, U.S. Army Coastal Eng. Res. Cent., Vicksburg, MS.

Church, J.C. and E.B. Thornton, 1993, Effects of breaking wave induced turbulence within a longshore current model, Coastal Eng., 20, 1-28.

Feddersen, F., R.T. Guza, S. Elgar, and T.H.C. Herbers, 1996, Cross-shore structure of longshore currents during DUCK94, 23rd Intern. Conf. on Coastal Eng., ASCE Orlando, FL, V.3, pp. 3666-3679.

Gable, C.G. (ed), 1981, Report on data from the Nearshore Sediment Transport Study experiment on Leadbetter Beach, Santa Barbara, California, January-February, 1980, IMR Ref, 80-5, Univ of Calif, Inst. of Mar. Resour, La Jolla, CA.

Garcez Faria, A.F., E.B. Thornton, T.P. Stanton, C.V. Soares, and T.C. Lippmann, 1998, Vertical profiles of longshore currents and related bed shear stresses and bottom roughness, J. Geophys. Res., V. 103, 3217-3232.

Holland, K.T., R.A. Holman, T.C. Lippmann, J. Stanley, and N. Plant, 1997, Practical use of video imagery in nearshore oceanographic field studies, IEEE J. of Oceanic Eng., V.22, N. 1, pp 81-92.

Hubertz, J.M., 1986, Observations of local wind effects on longshore currents, Coastal Engineering, V.10, pp. 275-288.

Komar, P.D., 1971, Nearshore cell circulation and the formation of giant cusps, Geol. Soc. Amer. Bull., V. 82, pp. 2643-2650.

Komar, P.D., 1979, Beach-slope dependence on longshore currents, Journal of Waterway, Port, Coastal, and Ocean Engineering, V. 105, pp. 460-464.

Komar, P.D. and J. Oltman-Shay, Nearshore currents, in Handbook of Coastal and Ocean Engineering, Vol. 2 edited by J.B. Herbich, pp. 651-680, Gulf Publishing Co., Houston, 1990.

Longuet-Higgins, M.S., 1970a, Longshore currents generated by obliquely incident waves, 1, J. Geophys. Res., V. 75, 6778-6789.

Longuet-Higgins, M.S., 1970b, Longshore currents generated by obliquely incident waves, 2, J. Geophys. Res., V. 75, pp 6790-6801.

Ludwick, J.C., 1978, Coastal currents and an associated sand stream off Virginia Beach, Virginia, J. Geophys. Res., 83, 2364-2372.

Lundberg, D.L., K.T. Holland, and J.C.Church, 1997, A semi-empirical longshore current model, NRL Memorandum Rep. NRL/MR/7442-97-8066, 38p.

Mettlach,T.R. and D.A. May, 1997, The accuracy of the Navy-Standard Surf Model-derived modified surf index and its sensitivity to nearshore bathymetric profile error, NRL Formal Rep. NRL/FR/7240--97-9665, 29p.

Putrevu, U., J. Oltman-Shay, and I.A. Svendsen, 1995, Effect of alongshore nonuniformities on longshore current predictions, J. Geophys. Res., V. 100 No. C8, pp. 16,119-16,130.

Thornton, E.B. and R.T. Guza, 1986, Surf zone currents and random waves: field data and models, J. Phys. Oceanog., V16, No. 7, pp. 1165-1178.

Reiners, A.J.H.M., E.B. Thornton, and T.C. Lippmann, 1995, Longshore currents over barred beaches, Coastal Dynamics, pp. 413-424.

Wu, C.S., E.B. Thornton, and R.T. Guza, 1983, Waves and longshore currents: comparison of a numerical model with field data, J. Geophys. res., V90 N. C3, 4951-4958.

Xu, J.P. and L.D. Wright, 1998, Observations of wind-generated shoreface currents off

Duck, North Carolina, J Coastal Res. V. 2 No. 2, pp 610-619.